

# Musculoskeletal applications of flat-panel volume CT

Benjamin Reichardt · Ammar Sarwar ·  
Soenke H. Bartling · Arnold Cheung ·  
Michael Grasruck · Christianne Leidecker ·  
Miriam A. Bredella · Thomas J. Brady · Rajiv Gupta

Received: 2 November 2007 / Revised: 21 January 2008 / Accepted: 3 February 2008 / Published online: 29 April 2008  
© ISS 2008

**Abstract** Flat-panel volume computed tomography (fpVCT) is a recent development in imaging. We discuss some of the musculoskeletal applications of a high-resolution flat-panel CT scanner. FpVCT has four main advantages over conventional multidetector computed tomography (MDCT): high-resolution imaging; volumetric coverage; dynamic imaging; omni-scanning. The overall effective dose of fpVCT is comparable to that of MDCT scanning. Although current fpVCT technology has higher spatial resolution, its contrast resolution is slightly lower than that of MDCT (5-10HU vs. 1-3HU respectively). We discuss the efficacy and potential utility of fpVCT in various applications related to musculoskeletal radiology and review some novel applications for pediatric bones, soft tissues, tumor perfusion, and imaging of tissue-engineered bone growth. We further discuss high-resolution CT and omni-scanning (combines fluoroscopic and tomographic imaging).

**Keywords** Musculoskeletal applications · Flat-panel volume computed tomography · High-resolution imaging · Trabecular imaging

---

B. Reichardt · A. Sarwar · A. Cheung · M. A. Bredella ·  
T. J. Brady · R. Gupta (✉)  
Department of Radiology, Massachusetts General Hospital,  
Harvard Medical School,  
55 Fruit Street, FND-216,  
Boston, MA 02114, USA  
e-mail: rgupta1@partners.org

S. H. Bartling  
Department of Medical Physics in Radiology, DKFZ,  
Heidelberg, Germany

M. Grasruck · C. Leidecker  
Siemens Medical Solutions,  
Forchheim, Germany

## Introduction

Despite all of the temporal and spatial resolution advances of CT over the past few years, the application of conventional CT in some areas of musculoskeletal radiology remain limited by spatial resolution. The current generation of CT scanners offers a maximum resolution of approximately  $0.5 \times 0.5$  mm in-plane and 0.5 to 1.0 mm in the z-axis direction [1]; however, this resolution is still below the limit for visualizing the minute trabeculae in bones, showing a coarse texture image rather than the fine structure of trabecular bone [2, 3]. One recent development in the potential to image minute, slender trabeculae is flat-panel volume CT (fpVCT). fpVCT uses digital flat-panel detectors and can provide ultra-high spatial resolution (up to  $150 \times 150$   $\mu\text{m}$ ) in 2-D projections [4]. The main advantages of this design are volumetric coverage, higher spatial resolution with isotropic voxel imaging and reduced metal and beam hardening artifacts [4].

The purpose of this article is to highlight the main features of a prototype fpVCT compared with a conventional MDCT scanner and describe potential refinements and advances in musculoskeletal imaging.

## Fundamentals of flat-panel volume CT

A fpVCT scanner combines advances in CT with digital flat-panel detector technology [5, 6]. This innovative system provides ultra-high isotropic spatial resolution ( $150 \times 150 \times 150$   $\mu\text{m}$ ) and the advantage of dynamic CT scanning with a wide-bore scanner. Besides the CT gantry-mounted flat-panel systems, there are other systems available with flat-panel detectors. These include bench-top systems that either have a fixed gantry with a rotating

stage or a rotating gantry with a stationary stage for small volumes of interest. There are machines available for large volume scanning that combine a C-arm gantry with flat-panel detectors. Another option for high-resolution scanning is micro-CT. A CT gantry-mounted flat-panel system, dubbed fpVCT, was used in the research described in this paper. Unlike micro-CT, which is limited by the size of the scanned volume, fpVCT is suitable for *in vivo* imaging of animals and humans [4]. By virtue of a slip-ring or other mechanisms for transmitting data from the rotating gantry to the stationary reconstruction computer, such systems are also capable of continuous imaging, a feature that C-arm-based systems do not provide.

The imaging chain of the prototype fpVCT used for this research consists of a modified X-ray tube, filters and beam-formers, collimator, and a digital flat-panel detector (40×30 cm), all mounted on a modified Sensation-16 CT gantry (Siemens Medical Solutions, Forchheim, Germany). The gantry is capable of rotating at a top speed of 0.4 s/rotation. However, the fpVCT system has not been tested at the highest possible angular speed due to a slow scintillator and the reduced numbers of projections collected per rotation. The current design is targeted to operate from 2 s to 20 s per rotation. As the gantry rotates, projection images of the anatomy are acquired. These 2-D projections are reconstructed into a volumetric stack of slices using a 3-D reconstruction algorithm (i.e., filtered back projection). Additionally, the imaging chain can be “parked” in one position to obtain fluoroscopic imaging from any arbitrary angle in space, or can be rotated continuously to visualize temporal evolution of a dynamic process. These features form the basis of its use as a proposed “omni-scanner” that combines X-ray fluoroscopy and computed tomography (CT) in one highly flexible system [7].

A cesium iodide (CsI) flat-panel detector is used in fpVCT to provide a matrix of 2,048×1,536 detector elements, each with a dimension of 194×194  $\mu\text{m}$ . The scintillator is deposited directly on the matrix of photo cells etched in order to provide intimate optical contact. This construction, when combined with the novel columnar structure of the CsI, serves to significantly enhance the efficacy with which the light from scintillation events is conveyed to the photo cells and preserved in the electronic image.

A flat-panel detector provides many scanning modes to optimize the fidelity of the projection data. With a 2×2 binning mode, which combines data from 4 neighboring pixels, the spatial frequency at 10% of the modulator transfer function (MTF) is 24 line-pairs per centimeter lp/cm. In contrast, with a 1×1 binning mode the spatial frequency at 10% of the MTF is 28 lp/cm. At the isocenter, with a

magnification factor of approximately 1:2, this translates into an effective pixel resolution of approximately 200×200  $\mu\text{m}$  for the 2×2 binning mode and 150×150  $\mu\text{m}$  for the 1×1 binning mode. Current clinical MDCT scanners, by comparison, offer approximately 500×500  $\mu\text{m}$  in plane resolution and 500–1,000  $\mu\text{m}$  resolution along the z-axis; a 74-fold difference in spatial resolution [1].

The fpVCT also employs a unique reconstruction algorithm, an adaptation of the 3-D Feldkamp algorithm. The 3-D nature of this algorithm ensures that each voxel, at least at the isocenter, has isotropic dimensions (i.e., 150×150×150  $\mu\text{m}$  for the 1×1 binning mode and 200×200×200  $\mu\text{m}$  for the 2×2 binning mode).

With respect to contrast resolution, fpVCT has the ability to differentiate structures with a difference of 5 HU over the background [8]. This is slightly inferior to MDCT, which can differentiate structures to within approximately 1 HU [9]. The difference is largely due to the lower dynamic range of the CsI-based flat-panel detector. However, this slight difference is not consequential in most MSK applications.

Given its high isotropic spatial resolution and its capabilities in volume acquisition, fpVCT appears to be a promising new imaging modality for studying fractures and other musculoskeletal pathology.

### Effective radiation dose

The effective dose is a function of the X-ray exposure, the length of the scan, and the body part being scanned. For fpVCT, the effective dose can be estimated from the Dose–Length Product (DLP). We measured the dose during a volumetric scan of a hand that included the wrist joint and the distal radius, utilizing the complete 18-cm panel. For a 20-s scan employing 80 kV, 30 mA, a 2×2 binning mode, and a 50% X-ray duty cycle, the DLP was measured to be 7.4 mGy × 18 cm = 133.2 mGy.cm. The effect on the body part being scanned is determined by a multiplication factor that takes into account the radio sensitivity of different organs. Since the extremities are relatively radio-insensitive, this factor for the hand is 0.0008 mSv/mGy.cm. Therefore, the effective dose for a single scan of the distal radius is 7.4 × 18 × 0.0008 = 0.11 mSv. By comparison, a PA chest radiograph, which is a medical examination with one of the lowest levels of radiation exposure, results in an effective dose of 0.02 mSv. Therefore, the effective radiation dose from a hand scan including the distal radius is equal to that of about 5 PA chest radiographs. This level of radiation exposure equals the dose an average person receives from natural background radiation over 10 to 12 days.

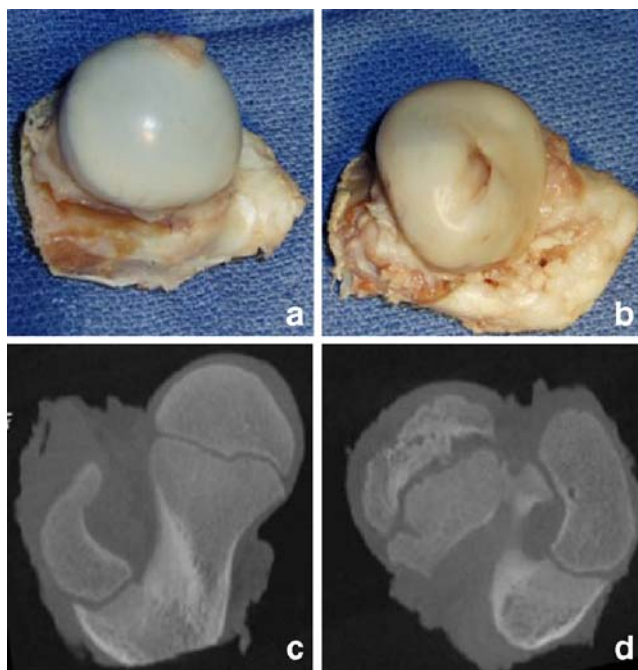


**Fig. 1** **a, b** Pathology specimens and **c, d** flat-panel volume computed tomography (fpVCT) images of the femoral head of a 6-week-old piglet. **a** and **c** depict a normal femoral head, while **b** and **d** show a similar femoral head subject to a model of Legg-Calvé-Perthes disease. (Image courtesy of Drs. Diego Jaramillo, Children's Hospital of Philadelphia, and Susan A. Connolly and Gleeson F. Rebello, Boston Children's Hospital)

### Musculoskeletal applications

There are four main advantages of fpVCT compared with MDCT:

1. High resolution
2. Volumetric coverage
3. Dynamic imaging
4. Omni-scanning (i.e., combined fluoroscopy and tomography)

The following discussion will describe the key attributes and potential applications of fpVCT.

The fpVCT scanner is a research prototype that has not yet been FDA-approved. Therefore, all imaging to date has been performed on animals or using ex vivo specimens from cadaver parts.

#### High-resolution imaging

Flat-panel volume computed tomography provides a spatial resolution of 150  $\mu\text{m}$ , which is better than MDCT by a factor of 3. Its contrast resolution of about 5 HU, however, is slightly inferior to that available on MDCT. Applications

that require detailed imaging of high contrast objects would appear to benefit the most from fpVCT. The following subsections present image examples of long bones, wrists/hands, knees, and ankles utilizing fpVCT.

#### Long bone imaging

Figure 1 shows a simulated animal model of avascular necrosis of the femoral head (Legg-Calvé-Perthes disease) in a 6-week-old piglet. The details of the pathology can clearly be seen on fpVCT images **c** and **d**) because of the high-resolution technique.

Figure 2 shows a sagittal and an axial view through a human femur specimen (courtesy of Axiom Lab, University of Erlangen, Germany). Scan parameters used were: 81 kV tube voltage, 398 projections, and 3.6  $\mu\text{Gy}$  of X-ray dose per projection. In order to enable high-resolution imaging, a focus spot size of 0.4 mm was used, with a source to detector distance of 1.2 m. The specimen was positioned so that the magnification ratio from the isocenter to the detector was 1.6. Different trabecular bands coursing through the femoral neck can be easily visualized as individual fibro-osseous strands. This degree of fine structural detail suggests that subtle cortical and trabecular disruption will be identified. Figure 2 was generated using a small focal spot and a C-arm gantry. We attempted to replicate these results in a clinical setting using a fast CT gantry and a slightly bigger focal spot size. Figure 3 shows a sagittal section through an arthritic knee using the prototype fpVCT, and a comparable image acquired using clinical MDCT (LightSpeed 16; GE Medical Systems, Milwaukee, WA, USA). The high definition of trabecular structure depicted by fpVCT suggests that subchondral impaction may be seen in the areas of cartilage loss.

Similarly, the high-resolution imaging shows details of metaphyseal corner fractures in cases of child abuse that were not visible on radiographs and MDCT in the ex vivo specimen. Figure 4 shows a 3-D rendering of distal tibia and fibula from a proven child abuse case. The classic

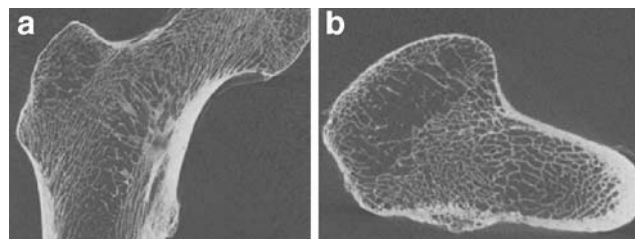


**Fig. 2** **a** Sagittal and **b** axial sections of a femur specimen using a flat-panel imager mounted on a C-arm (DynaCT; Siemens Medical Systems, Erlangen, Germany). Image courtesy of Dr. Willi Kalendar, University of Erlangen, Germany



**Fig. 3** Coronal sections through an ex-vivo human knee using **a** flat panel volume computed tomography (fpVCT) and **b** multidetector computed tomography (MDCT) scanners. Note the improvements in trabecular definition and partial volume averaging on the fpVCT image due to the higher spatial resolution and isotropic nature of its voxels

bucket handle fracture can be seen in these two views. Note the bucket handle configuration in the top left hand image, from which these fractures derive their name. Contrary to what some might mistakenly believe [10], these fractures are not periosteal sleeve avulsions. Instead, they are transverse fractures that span the full thickness of the bone at the zone of provisional calcification, a location where the growing bone is the weakest. The longitudinal fpVCT image shown in Fig. 4b clearly demonstrates this finding.

#### Hand and wrist imaging

Two questions about the clinical utility of fpVCT images remain:

- Does improved spatial resolution actually translate into better detection of lesions?
- Is the contrast resolution adequate for imaging soft tissue lesions?

While a clinically acceptable answer to these questions will require a controlled trial, one can get a sense of the possible results through simulated lesions. To this end, a hand from an embalmed cadaver was severed at mid-forearm level and a set of lesions simulating laceration,

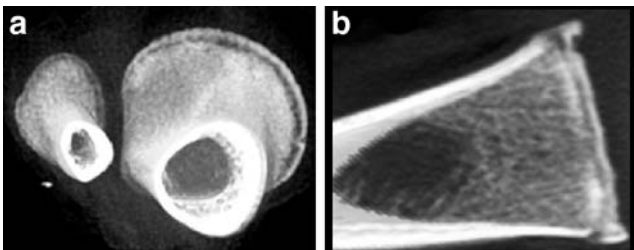


**Fig. 4** **a, b** High-resolution maximal intensity pixel (MIP) renderings of a classical metaphyseal fracture, also known as a corner fracture or bucket handle fracture, from a child abuse victim. **a** shows the “bucket handle” from which this fracture derives its name. **b** shows that despite the appearance of a periosteal avulsion fracture, the lesion is actually a transverse fracture involving the entire width of the bone. (Specimens courtesy of Dr. Paul Kleinman, Boston Childrens Hospital)

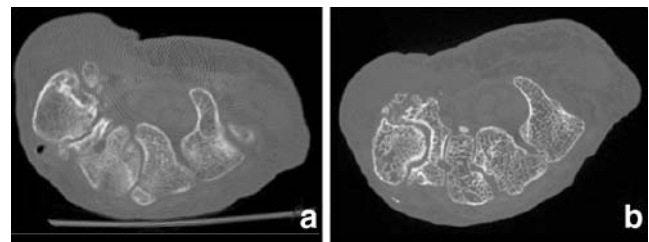
blunt trauma, piercing trauma, hairline bone fractures, a cut in the dorsal expansion, cuts in the pulley system of the phalanges, and bone pathology were created. The specimen with these lesions was scanned with the fpVCT and MDCT (GE LightSpeed) scanners using routine clinical protocol.

In a cross-section through the human wrist (Fig. 5), the bony matrix was better visualized using fpVCT images. Any lesion that distorted the architecture of the bone matrix, the cortex, or the soft tissue around it, was more clearly seen using fpVCT than MDCT.

The contrast resolution using fpVCT was sufficient to demonstrate individual components of the joint (bone cortex and insertion of the tendons; Fig. 6). In addition, fpVCT enabled direct visualization of the digital sheath and the pulleys. In fpVCT images, we were able to directly visualize these structures and identify the three lesions we had created in them. Lacerations in the tendons, one of the most common injuries of the hand, could be directly visualized (Fig. 7).

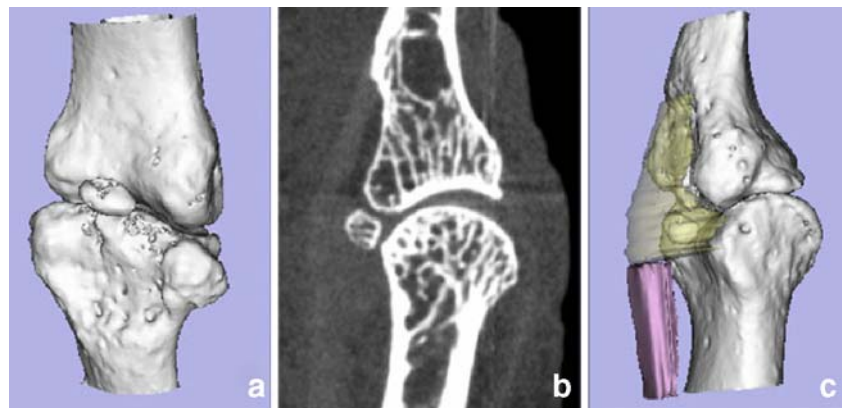
In addition to soft tissue injuries, fpVCT also shows improvement compared with current technology in the detection of clinically important skeletal injuries. While numerous studies have shown the utility of regular radiographs and MDCT for the evaluation of skeletal fractures, these technologies are limited in their ability to show trabecular regrowth and bridging. This is essential and direct sign of the healing process [11–13]. This is especially important in bones such as the scaphoid, where the blood supply is tenuous and delayed, or missed diagnosis of non-unions might lead to formation of scaphoid non-union advanced collapse (SNAC) and early onset arthritis [14, 15]. In this respect, Fig. 8 shows axial and coronal images along the scaphoid bone. Fig. 8a and b depict normal bone structure, whereas c and d clearly show a fine fracture and fragmentation of the scaphoid bone.

Figure 9 shows a section through the carpal tunnel rendered so that both bony as well as soft-tissue structures can be visualized. The break in the flexor retinaculum and all the tendons are clearly shown. The dorsal aspect of a dissected hand can be seen with 3-D rendering in Fig. 9. The trabecular structure of the bones can be appreciated on these fpVCT images. Note that on both of these images, the



**Fig. 5** Comparison of an axial image through the proximal carpal row using **a** MDCT and **b** fpVCT. fpVCT clearly shows the micro-architecture of the trabecular bone

**Fig. 6** **a, c** Three dimensional reformatted and **b** sagittal images of the distal interphalangeal joint of the first digit using fpVCT. The flexor tendon (*pink*) merges into the posterior part of the joint capsule (*yellow*)



contrast resolution is sufficient to clearly show soft tissue detail.

Because of their smaller voxel size, fpVCT imaging produces fewer metal artefacts compared with MDCT. This is demonstrated in Fig. 10, where a titanium screw was placed adjacent to one of the tendons. As can be seen in this image, no metal artefacts are evident and there is no image degradation.

#### *Imaging of tissue-engineered bone*

The ability of fpVCT to acquire high-resolution CT images makes it useful in nondestructive testing. These applications demand high-resolution information from interior structures without destroying the specimen. We have tested

one such application in our research on tissue engineering, where the progress of bone growth needs to be accurately tracked over time.

This was successfully done in studies examining tissue-engineered bone growth using special hydrogels [16–18]. Initially, high-resolution 3-D images of a human thumb were acquired by fpVCT and used to create a 3-D print out. The 3-D model was then used as scaffolding on which human mesenchymal cells were placed. This preparation was implanted under the skin of a nude mouse. The investigators were able to confirm in vivo formation of bone-like tissue 15 weeks after placing human mesenchymal stem cells [17]. This result was achieved using Hounsfield unit values acquired with fpVCT. Thus, the high detail provided by fpVCT was crucial in the serial assessment of bone growth, without euthanizing the animal or removing the scaffolding from its in vivo environment.



**Fig. 7** **a** fpVCT and **b** anatomical preparation of the flexor tendons after simulated trauma inflicted on a cadaveric hand. This image clearly shows the ability of fpVCT to detect soft tissue lesions (*black arrows*), despite the lower contrast resolution

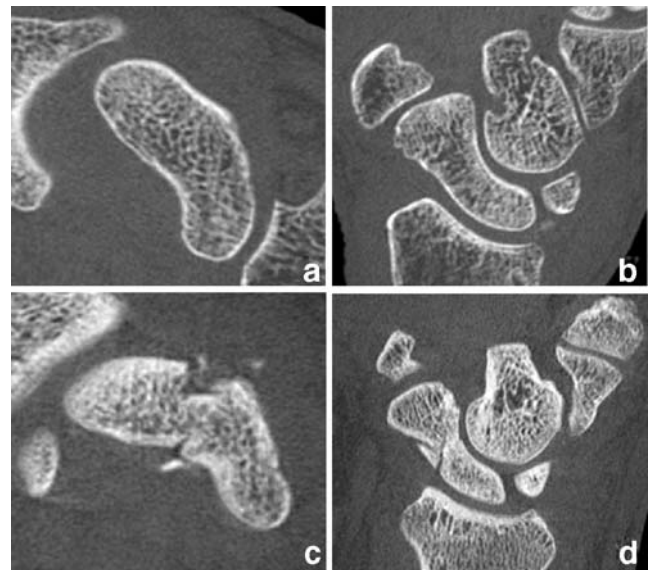


**Fig. 8** Images oriented along the **a, c** axial and **b, d** coronal planes of the scaphoid bone. The *top row* shows a bone without a fracture and the *bottom row* shows a displaced fracture of the scaphoid seen on fpVCT



**Fig. 9** Axial section through the proximal carpal row showing the carpal tunnel with its distal pillars. A laceration in the flexor retinaculum can be seen (*white arrow*)

### Volumetric coverage

The size of the flat panel along the axial dimension (i.e., along Z) is 30 cm. This translates into a field of view (FOV) of about 18 cm along the z-axis. For comparison, the traditional 16- or 64-row CT scanners have a FOV of about 2–4 cm. Thus, both projection and tomographic views of entire organs or pathologies are possible using fpVCT.

Volumetric acquisition and complete organ coverage are another major advantage of fpVCT. To acquire these images, a rabbit was anesthetized and a peripheral IV line was started in an ear vein. The 3-D images (Fig. 11) from the resulting datasets demonstrate excellent image quality and wide coverage available from a single rotation of the scanner. Even with non-optimized injection time, fpVCT was able to show fine skeletal and vascular details in the head, neck and pelvis of the animals imaged. This feature of fpVCT provides a major improvement compared with conventional high-resolution scanners, such as micro-CT, where the small FOVs preclude imaging of large subjects.

**Fig. 10** Dorsal aspect of a volume-rendered, dissected specimen showing excellent soft tissue detail adjacent to high contrast objects on fpVCT images. Note the lack of metal artefacts from the screw implanted next to the tendon of the extensor pollicis longus (*black arrow*)

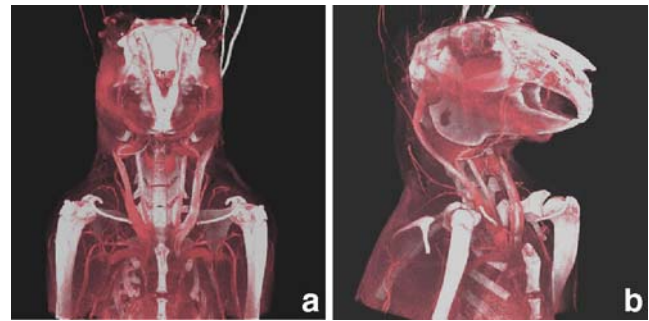


**Fig. 11** Frontal (**a**) and lateral (**b**) volume-rendered images of a head and neck angiogram of a rabbit. The entire image was acquired with one rotation of the gantry without table movement. It clearly highlights the unique ability of the fpVCT to acquire high resolution images of a large field of view

### Dynamic imaging

In addition to the above features, fpVCT also allows dynamic imaging of time-varying processes. The ability of fpVCT to cover a large volume during one rotation, together with the relatively short rotation times and the ability to rotate continuously, allows observation of changes in tissue characteristics over a period of time. If the temporal resolution is short enough, the evolution of a contrast bolus can be followed through the vessels, soft tissue, and bone. fpVCT for animal skeleton imaging [19], tumor angiogenesis [20], perfusion studies [19], and lung parenchyma [21] have been described. Using such a dataset, a perfusion study of these tissues can be performed, making it possible to combine CT angiography and CT perfusion in one dynamic imaging process. In addition, the larger scan FOV of fpVCT makes it possible to scan animals larger than rodents, even primates. To demonstrate this, four rabbits underwent an implantation of VX-2 cancer tissue. Six weeks after implantation in the right and left femoral bone, we performed tumor perfusion angiography. Figure 12 shows six sequential 3-D images of the vascular supply of the artificially created tumor.

The visualization of the arterial supply of a large muscular tumor can help in assessing operability for removal. Additionally, visualization of the blood supply prior to the operation can help in the optimal planning of the procedure.

### Omni-scanning

In current clinical practice, three different radiologic modalities—radiography and fluoroscopy (R&F), X-ray angiography, and computed tomography (CT)—play a central role. Although all these modalities are based on X-ray imaging, they provide different and often complementary information about a disease process. These three X-ray modalities have remained discrete—even though at a block diagram level they seem to utilize similar

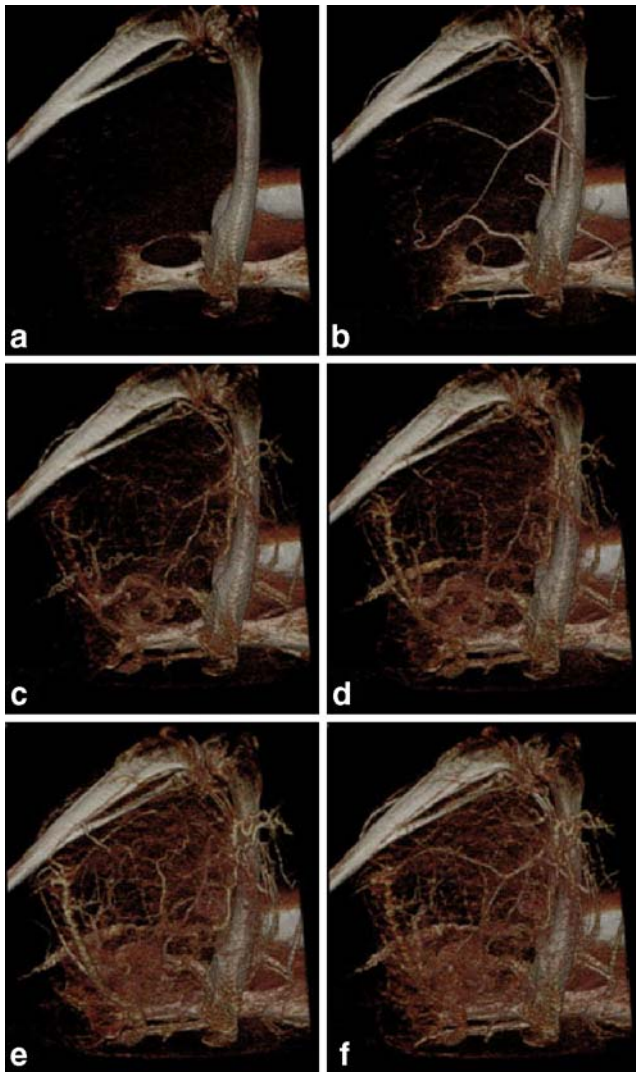


**Fig. 12** Volume-rendered image of an artificially created VX-2 tumor in a rabbit model. Each panel is taken at a different time-point, with time increasing from **a** to **f**. Changes in tumor perfusion over time from the early arterial to the late venous phase are clearly depicted

components—primarily because of detector technology. R&F- and C-arm-based systems require a detector that can provide 2-D projections at the video frame rate. Consequently, these systems use image intensifiers for image capture at the video frame rate of 25–30 frames/s. This allows for fast, real-time image capture, but the dynamic range of the data is limited to 8–10 bits/pixel. Consequently, only high-contrast structures such as opacified vessels and bones can be visualized.

On the other side of the spectrum, the detectors used for computed tomography have a very high dynamic range. This enables contrast resolution of almost 256,000 shades of gray (i.e., a dynamic range of 18 bits) at the detector level. Also, the detector panel can be read out at an incredibly fast frame rate: in one rotation lasting about 0.4 s, approximately 1,000 projections are acquired and

read out. The CT detector elements are bigger, measuring approximately 1 mm in their smallest dimension. These detectors are not available for large area arrays, and they are made long in the axial dimension to provide better sensitivity, which leads to anisotropic volumetric data.

Flat-panel volume CT that employs the recently developed flat-panel detectors could potentially reconcile the divergent demands of these three different X-ray modalities, which would be a significant leap forward.

#### Intra-operative imaging and navigation

The potential omni-scanning capability of fpVCT, together with its potential use as a C-arm makes it an ideal modality for intra-operative imaging. Flat-panel detectors mounted on a C-arm provide a highly mobile and flexible scanning arrangement [22, 23]. These systems, which provide both projection and tomographic imaging, have applications in maxillofacial and skull base surgery [22]. In these applications, the accuracy of intra-operative imaging greatly benefits from the higher resolution of fpVCT in comparison to MDCT.

#### Other developments

Real-time fpVCT volume reconstruction that is combined with continuous data acquisition, namely CT fluoroscopy, could be developed to provide real-time information during surgery or interventions. Further, dynamic CT information could be delivered in real time.

#### Conclusion

The simple experiments outlined above demonstrate that fpVCT provides excellent visualization of bony anatomy and pathology. FpVCT shows vessels, tendons, and nerves in great detail, and the contrast resolution is not found to be a limiting factor. Any lesion that distorts the architecture of the bone matrix, or the soft tissue around it, is visualized in fine detail. Further, in fpVCT the image quality was independent of the orientation of reformatted slices, due to the isometric voxel size.

In short, the fpVCT provides a comprehensive imaging platform that allows for X-ray, fluoroscopic and tomographic scanning. These scans have the benefit of being high resolution, covering a large tissue volume of interest, imaging at different time points to assess dynamic changes and finally, to provide real-time fluoroscopy for interventional procedures. As shown, these features make fpVCT ideally suited for certain research applications while further developments hold considerable promise for its use as a combined machine for CT and fluoroscopy.

**Acknowledgments** The authors wish to thank Drs. Willi Kalendar, Diego Jaramillo, Susan A. Connolly, Gleeson F. Rebello, and Paul Kleinman for the use of their images.

## References

- Flohr TG, Stierstorfer K, Ulzheimer S, Bruder H, Primak AN, McCollough CH. Image reconstruction and image quality evaluation for a 64-slice CT scanner with z-flying focal spot. *Med Phys* 2005; 32: 2536–2547.
- Link TM, Majumdar S, Lin JC, et al. A comparative study of trabecular bone properties in the spine and femur using high resolution MRI and CT. *J Bone Miner Res* 1998; 13: 122–132.
- Link TM, Vieth V, Stehling C, et al. High-resolution MRI vs multislice spiral CT: which technique depicts the trabecular bone structure best? *Eur Radiol* 2003; 13: 663–671.
- Gupta R, Grasruck M, Suess C, et al. Ultra-high resolution flat-panel volume CT: fundamental principles, design architecture, and system characterization. *Eur Radiol* 2006; 16: 1191–1205.
- Kotter E, Langer M. Digital radiography with large-area flat-panel detectors. *Eur Radiol* 2002; 12: 2562–2570.
- Kalendar WA. [The use of flat-panel detectors for CT imaging]. *Radiologe* 2003; 43: 379–387.
- Gupta R, Jones SE, Mooyaart EA, Pomerantz SR. Computed tomographic angiography in stroke imaging: fundamental principles, pathologic findings, and common pitfalls. *Semin Ultrasound CT MR* 2006; 27: 221–242.
- Nikolaou K, Flohr T, Stierstorfer K, Becker CR, Reiser MF. Flat panel computed tomography of human ex vivo heart and bone specimens: initial experience. *Eur Radiol* 2005; 15: 329–333.
- Shin HO, Falck CV, Galanski M. Low-contrast detectability in volume rendering: a phantom study on multidetector-row spiral CT data. *Eur Radiol* 2004; 14: 341–349.
- Kleinman PK, Marks SC, Blackburne B. The metaphyseal lesion in abused infants: a radiologic-histopathologic study. *AJR Am J Roentgenol* 1986; 146: 895–905.
- Sehat KR, Bannister GC. The prevalence of established scaphoid fracture non-union found on incidental radiography. *Injury* 2000; 31: 275–276.
- Tiel-van Buul MM, Roolker W, Verbeeten BW, Broekhuizen AH. Magnetic resonance imaging versus bone scintigraphy in suspected scaphoid fracture. *Eur J Nucl Med* 1996; 23: 971–975.
- Frahm R, Lowka K, Vinec P. [Computerized tomography diagnosis of scaphoid fracture and pseudarthrosis in comparison with roentgen image]. *Handchir Mikrochir Plast Chir* 1992; 24: 62–66.
- Martini AK, Schiltenswolf M. [Changes in the wrist joint in spontaneous course of scaphoid pseudarthrosis]. *Handchir Mikrochir Plast Chir* 1995; 27: 201–207.
- Stahelin A, Pfeiffer K, Sennwald G, Segmuller G. Determining carpal collapse. An improved method. *J Bone Joint Surg Am* 1989; 71: 1400–1405.
- Weinand C, Gupta R, Huang AY, et al. Comparison of hydrogels in the in vivo formation of tissue-engineered bone using mesenchymal stem cells and beta-tricalcium phosphate. *Tissue Eng* 2007; 13: 757–65.
- Weinand C, Gupta R, Weinberg E, Madisch I, Jupiter JB, Vacanti JP. Human shaped thumb bone tissue engineered by hydrogel-beta-tricalciumphosphate/poly-epsilon-caprolactone scaffolds and magnetically sorted stem cells. *Ann Plast Surg* 2007; 59: 46–52; discussion 52.
- Weinand C, Pomerantseva I, Neville CM, et al. Hydrogel-beta-TCP scaffolds and stem cells for tissue engineering bone. *Bone* 2006; 38: 555–563.
- Knollmann F, Valencia R, Buhk JH, Obenauer S. [Characteristics and applications of a flat panel computer tomography system]. *Rofo* 2006; 178: 862–871.
- Kiessling F, Greschus S, Lichy MP, et al. Volumetric computed tomography (VCT): a new technology for noninvasive, high-resolution monitoring of tumor angiogenesis. *Nat Med* 2004; 10: 1133–1138.
- Marten K, Engelke C, Grabbe E, Rummeny EJ. [Flat-panel detector-based computed tomography: accuracy of experimental growth rate assessment in pulmonary nodules]. *Rofo* 2004; 176: 752–757.
- Rafferty MA, Siewerdsen JH, Chan Y, et al. Investigation of C-arm cone-beam CT-guided surgery of the frontal recess. *Laryngoscope* 2005; 115: 2138–2143.
- Siewerdsen JH, Moseley DJ, Burch S, et al. Volume CT with a flat-panel detector on a mobile, isocentric C-arm: pre-clinical investigation in guidance of minimally invasive surgery. *Med Phys* 2005; 32: 241–254.